*Journal of Fluids and Structures* (1999) **13,** 647–661
Article No.: jfls.1999.0223 available online at http://www.idealibrary.com on IDEAL

# VORTEX RING RECONNECTION IN LASER–MATTER INTERACTIONS

S. LUGOMER

*Ruđer Bošković Institute, Bijenička c. 54, 10001 Zagreb, Croatia*

(Received 2 March 1998 and in revised form 4 December 1998)

Laser-induced microscale vortex rings have been generated on a vaporizing tantalum surface, and their reconnection was studied in the presence of the shock waves on the nanosecond (ns) time scale. A reach spectrum of the ring structures was obtained, some of which have been observed for the first time. Qualitatively, three classes of interactions were distinguished, on the basis of relative relation between the shock momentum $P_S$ and momentum of the circulating fluid $P_C$: interactions in the presence of low-momentum shock waves ($P_S < P_C$); interactions in the presence of the shock waves with momentum comparable to the momentum of a circulating fluid ($P_S \approx P_C$); and interactions in the presence of the shock waves of momentum larger than momentum of the circulating fluid ($P_S > P_C$). A matrix formalism was introduced for description of the reconnection process which assumes the reconnection as the transition between various states, and which automatically gives the time ordering of the processes, as well as the degeneracy of the states. 

## 1. INTRODUCTION

LASER-MATTER INTERACTIONS (LMI) at the short time scale (pulse duration), $\tau < 30$ ns, were shown to be almost ideal for the study of the vortex filament generation and self-organization (SO). The studies performed by our group in the regime of transition from planar-to-volume vaporization, at $\tau = 10$ ns, have shown the spontaneous formation of open- and closed-loop vortex filaments, showing various levels of the organization complexity (Lugomer 1996, 1997; 1998a,b).

Continuing the series of studies, this paper deals with generation of the microscale vortex rings and their interactions, especially with collision, reconnection and breaking, as a non linear and nonequilibrium process with strong dissipative character.

The processes taking place in the above-mentioned regime of LMI, are numerous and very complex. The first of them relates to the generation of vortex rings in the explosive decomposition of a spinodal fluid (liquid Ta) into a gaseous phase on the time scale $\leq 10$ ns. The spinodal fluid (Samokhin 1998; Samokhin & Uspensky 1997) is generated during surface superheating of metals in high-power, short-time-scale laser–metal interactions when the surface layer behaves as a dielectric. It thus becomes transparent, enabling a deep volume absorption of the laser beam. The vapour pressure above the surface prevents boiling, and causes superheating of the liquid metal (Lugomer 1996; Samokhin 1998, Samokhin & Uspensky 1977). The system is pushed into a metastable region of a thermodynamic diagram, where thermal conductivity $k \to 0$, and specific heat $C_p \to \infty$ (Lugomer 1996). The system is not stable, and exists only for a short time, after which it decomposes into a gaseous phase through microexplosions of surface bubbles, characteristic of the onset of the "volume" boiling. As usually assumed, this transition occurs at $Q \cong 10^8$ W/cm$^2$.

0889–9746/99/050647 + 15 $30.00 

The second process relates to the explosion of bubbles on the vaporizing surface which generates vortex filaments organized into spatial structures, ranging from circular (vortex rings) to very complex, and even to chaotic ones. The vortex ring, as the most simple structure, exhibits a rotation of each vertical element around the curved axis of the figure. The flow of the subsurface fluid separates at the edge of the explosion crater; a cylindrical vortex sheet forms, and rolls up into a vortex ring. The fluid velocity associated with microexplosions is comparable with the velocity of the expelled vapour in laser-driven vaporization, $v \sim 10^5$–$10^6$ cm/s, which gives high Reynolds numbers, Re $\sim 10^3$–$10^4$. Similar Reynolds numbers were obtained in experiments under highly controlled conditions (Reed 1988; Widnall & Sullivan 1973). Once formed, vortex rings behave as the independent entities which freely and easily move in the background fluid (surface molten layer).

Another group of processes, characteristic for the high-power laser–matter interactions on the short time scale, relates to the generation of the shock waves. They travel in all directions and being reflected from the sidewalls (of the small sample) they reverberate thorugh the sample, causing the interaction with surface hydrodynamic structures (vortex rings). The momentum transferred from the shock wave to the vortex ring causes its collision with other rings, the result of which is their interaction (Lugomer 1996, 1998; Lugomer & Maksimovic 1997.

The third group of processes is therefore the vortex ring interaction, the most important of which is the vortex ring reconnection. Two vortex rings, free to move come into contact and merge into a single ring, what is called the vortex connection. The vortex ring may then split to form new vortex rings, which is what is called *reconnection* (Kida *et al.* 1989). The reconnection process that starts on two closed rings, occurs—in a topological sense—by the foliation on a torus (Tamura 1976). This process is possible under the condition of torus stability, and under the condition that foliation establishes the "coherent neighbourhood", for any locally foliated manifold. Reconnection is an indication of dominance of dissipative effects over the coherence of structures. The topological changes and a dramatic change of fluid patterns occur on a small time-scale compared to evolution (Ricca & Berger 1996). From a dynamical point of view, reconnections take place when the vector field lines (vortex lines), cross each other. If two field lines meet, the point of crossing is a true nodal point. Dissipative effects allow the reconnection to proceed through such points. Vortex ring reconnections have been studied intensively from both theoretical and experimental points of view. The theoretical approach is generally based on the Biot–Savart model of vortex filaments which provides initial conditions for a finite-difference scheme for the incompressible Navier–Stokes equation (Asthurst & Meiron 1987).

Approaching motion of the vortex rings may be caused by the Biot–Savart law as assumed in numerical simulations of Oshima & Izutsu (1988), Kida *et al.* (1989), Pumir & Kerr (1987), Asthurst & Meiron (1987), but also by the surface shock waves, which is the dominant case in laser-material interactions. Vortex ring reconnections are difficult to be produced experimentally, and in principle they are limited to jets and to brief discharges of fluid from an orifice (Fohl & Turner 1988). However, in laser–metal interactions they appear spontaneously and, because of ultrafast cooling after pulse termination, they stay frozen permanently, thus enabling *a posteriori* analysis (Lugomer 1996).

## 2. THE EXPERIMENTAL SYSTEM

A $Q$-switched Nd:YAG laser of $Q \sim 10^7$ W/cm$^2$, ($Q < Q_{vb}$), of pulse duration $\tau = 10$ ns and of the spot size $2d \sim 3$–$4$ mm, was used for generation of vortex rings in the interaction space. Tantalum samples of $1 \times 1 \times 0{\cdot}05$ cm in size were mechanically polished and cleaned with alcohol. The surface analysis was done by optical and scanning electron

microscopes. The micrographs have been numerically filtered by using the Adobe Photoshop program.

## 3. RESULTS AND DISCUSSION

As mentioned in Section 2, laser-generated shock waves travel from the centre of the spot toward its periphery; from the periphery toward the centre, and finally, between the front and back side of the sample (O'Keefe *et al.* 1973). Their constructive interference at one point and destructive one at another point and dispersion generate an inhomogeneous shock- wave field with strong influence on the vortex ring dynamics and their mutual interactions. Consequently, vortex ring interactions belong to different classes present in various regions of the spot. Their classification is based on the relative magnitude of momentum of the circulating fluid, $P_C$, and momentum of the shock wave, $P_S$. Qualitatively, we distinguish a class of interactions in the presence of the low-momentum shocks or in their absence ($P_S < P_C$); a class of interactions in the presence of shock waves of momentum comparable to momentum of the circulating fluid ($P_S \approx P_C$) which disturbs the reconnection process by deformation of the vortex ring; and a class of interactions in the presence of high momentum shock waves ($P_S > P_C$), which cause breaking of the cross-linked rings.

### 3.1. Case of ($P_S < P_C$)

#### 3.1.1. *General considerations*

The cross-linking interaction of two vortex rings follows the scenario described by Fohl and Turner (1988) based on experimental observations and by Kida *et al.* (1989) and Oshima & Izutsu (1988) based on the numerical simulations.

Two ring vortices are located in close vicinity at an angle, Figure 1. The vorticity is distributed parallel to the centrelines of the vortex rings and distributed counterclockwise for one ring and clockwise for another one. Within each cross-section, vorticity is given by the Gaussian form (Kida *et al.* 1989)

$$\omega(r) = \omega_0 \exp\left(\frac{-r^2}{\sigma^2}\right), \tag{1}$$

where $r$ is the distance from the core centre, and $\omega_0$ and $\sigma$ (core size) are constants. The circulation $\Gamma$ of each ring is $\pi\omega_0\sigma^2$ (Kida 1989). Figure 1(a) corresponds to the initial phase of reconnection when two rings touch each other. They disappear at the point of contact by annihilation of vorticity of opposite sign. Then follows merging of the two rings into a single distorted ring by "cut-and-connect" (Kida *et al.* 1989; Oshima & Izutsu 1988).

Figure 1(b) corresponds to the second phase of the reconnection scenario, where the vortex tube with a saddle profile is formed with increasing radius of curvature. The two antiparallel portions of the saddle approach each other as they are straightened (Kida *et al.* 1989; Oshima and Izutsu 1988). As they become straight their approach is stopped before contact is established. Another reconnection process happens in this moment; the new "bridges" appear on the front side of the vortex tube at the border between the straight and circular parts of the tube. As a result, a merged vortex tube changes topologically into two rings connected by two "legs", which represents the third phase of the reconnection scenario. The cross-linked rings seen in Figure 1(c), can be attributed to the third phase, with the bridges on the rings established and with the leg-tubes significantly straightened.

More complex structures, also corresponding to phase 3, consisting of two knotted rings cross-linked with the third one, as can be seen in Figure 1(d). This structure (observed for

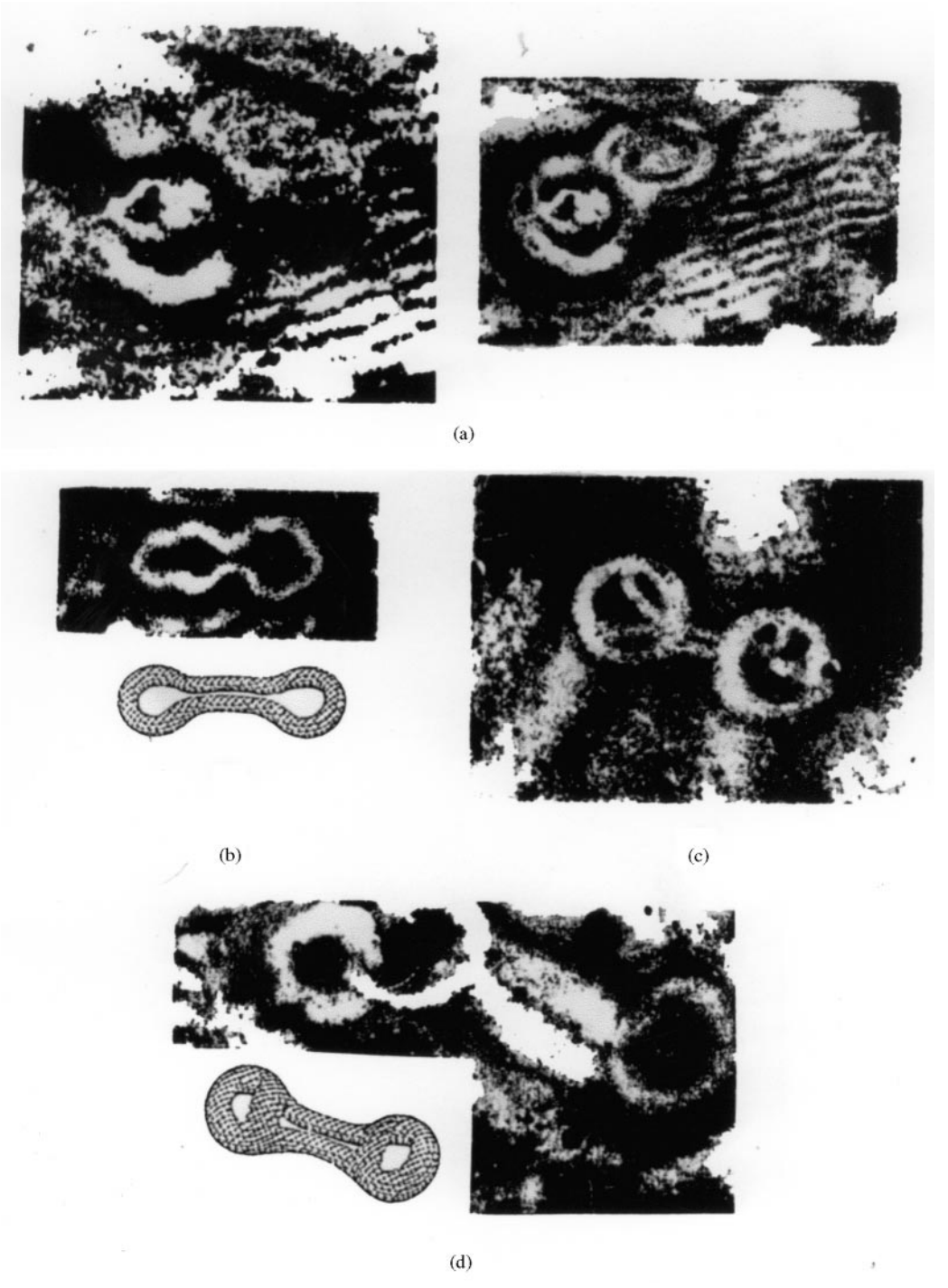


Figure 1(a–d). Caption on next page.

the first time) represents a ring with the Hopf bifurcation cross-linked with the other ring and indicates the chain of events which are time-ordered. Time ordering relates to the fact that the vortex ring must first bifurcate generating the Hopf link (knotted knot) (Lugomer 1997), and then it may establish the cross-linking with another ring in its vicinity (the reverse process is not possible, for purely topological reasons). This, at the same time indicates that the fastest process which occurs first has a lower order of complexity and then follows a slower one of a higher order of complexity. Thus, this ordering is two-fold: according to increasing order of topological complexity and according to decreasing process rate.

3.1.2. *Description of the reconnection by a matrix formalism*

The open-loop and the closed-loop vortex filament structures are usually described by the skein relations, i.e., by the recursion relations relating the knot invariants of knots whose diagrams are identical (Jones 1990; Wu 1992). Another way of description is based on the Alexander polynomials relating the knot invariants of the oriented knots and, finally, vortex rings and other knotted and unknotted vortex filaments can be described by the Jones polynomials, based on the braid group representation (Wu 1992).

However, reconnection of the vortex filaments of the open-loop or of the closed-loop type is a more difficult problem.

As a local process, reconnections are difficult to describe and are still a puzzle for theorists. One simple mathematical approach, which must be mediated by detailed knowledge of the particular physical process, involves techniques of "oriented surgery", performed on the bundle of constitutive vector field lines (strands). When two strands of the bundle come into contact, vector lines of one strand may recombine with vector lines of the other by a "cut-and-connect" process. The effect is local, but its consequences are global (on the topology). When this happens, we have a complete change of the topology of the system. (Ricca & Berger 1996).

Instead of following the above way of description we introduce new, very simple one, based on matrix formalism. We assume the vortex rings, unknotted and knotted ones (Hopf link) as well as the reconnected rings ..., to be the *states* of the organized circulating flow, described by the corresponding matrices. Instead of consideration of the processes "cut-and-connect" we consider the *transition between two states*. Transition between two states is described by the action of the particular operator $\mathcal{O}$, on the matrix of the particular state.

The above ring structures [shown in Figure 1(a–d)] may be symbolically described as follows: we assume the ring configurations to be a states, denoted $X$, $Y$, $Z$, $W$ and $K$, as schematically shown in Figure 1(e). The states $X$ and $X'$ correspond to the clockwise and counterclockwise rotation and can be represented by the $3 \times 3$ matrices $\mathbf{X}$ and $\mathbf{X}'$,

Figure 1. Reconnection of two vortex rings on liquid Ta surface without presence of the shock waves. (a) Two rings in the instant of touching Magnification $M \sim 2300\times$. Numerical filtering reveals thinning of the rings around the touching point, which corresponds to the initial phase of reconnection. (b) Two rings after first reconnection, which corresponds to the second phase of reconnection; $M \sim 1600x$. [Numerically generated corresponding form is given, for comparison; of from Oshima & Izutsu (1988)]. (c) Two rings after second reconnection, corresponding to the third phase of reconnection; $M \sim 1800\times$. Long, stretched leg-tubes are clearly seen. (d) Two rings with the Hopf link, cross-linked with the third one, corresponding to the phase 3 of reconnection. Flattening of both leg-tubes indicates diffusive spreading and core deformation because of interaction with the background fluid. [Numerically generated corresponding form is given for comparison; from Oshima & Izutsu (1988)]

respectively:

$$\mathbf{X} = \begin{pmatrix} 1 & 0 & 0 \\ 0 & 1 & 0 \\ 0 & 0 & 1 \end{pmatrix}, \quad \mathbf{X}' = \begin{pmatrix} 0 & 0 & -1 \\ 0 & -1 & 0 \\ -1 & 0 & 0 \end{pmatrix}. \tag{2}$$

The structure of the matrices $\mathbf{X}$ and $\mathbf{X}'$ indicates that the states $X$ and $X'$ are mirror states: the ring with right rotation is transferred into the ring with the left rotation by the mirror plane [Figure 1(e)].

The state $Y$ is a Hopf link represented by the matrix

$$\mathbf{Y} = \begin{pmatrix} 1 & 0 & -1 \\ 0 & -1 & 0 \\ -1 & 0 & 1 \end{pmatrix}.$$

It can be obtained from the state $X$ by the operation

$$\mathbf{Y} = \mathcal{O}_1 \mathbf{X},$$

where $\mathcal{O}_1$ is the operator

$$\mathcal{O}_1 = \begin{pmatrix} 1 & 0 & -1 \\ 0 & -1 & 0 \\ -1 & 0 & 1 \end{pmatrix}. \tag{3}$$

The structure of the $\mathbf{Y}$ matrix indicates that the $Y$ state lies not on one, but two planes. [The Hopf link is usually represented by two rings that lie in two perpendicular planes, Figure 1(e)].

The state $Z$ (corresponding to the cross-linked rings of clockwise and counterclockwise vorticity), is represented by the matrix

$$\mathbf{Z} = \begin{pmatrix} 1 & 0 & 1 \\ 0 & 0 & 0 \\ 1 & 0 & 1 \end{pmatrix}$$

and obtained by the operation

$$\mathbf{Z} = \mathrm{O}_2(\mathbf{X} \cdot \mathbf{X}'),$$

where

$$\mathcal{O}_2 = \begin{pmatrix} -1 & 0 & -1 \\ 0 & 0 & 0 \\ -1 & 0 & -1 \end{pmatrix} \tag{4}$$

The symmetric matrix $\mathbf{Z}$ indicates that the state $Z$ comprises one mirror plane; the vertical one, as can be seen in Figure 1(e).

The states $X$, $Y$ and $Z$ are the basic states, while $W$ and $K$ are the combined states obtained by the action of the operators $O_1$ and $O_2$ on the matrices $\mathbf{X}$ and $\mathbf{X}'$:

$$\mathbf{W} = \mathcal{O}_2\{[(\mathcal{O}_1\mathbf{X})\mathbf{X}'] = \begin{pmatrix} -2 & 0 & 2 \\ 0 & 0 & 0 \\ -2 & 0 & 2 \end{pmatrix} = 2\begin{pmatrix} -1 & 0 & 1 \\ 0 & 0 & 0 \\ -1 & 0 & 1 \end{pmatrix} \tag{5}$$

and

$$\mathbf{K} = \mathcal{O}_2\{[(\mathcal{O}_1\mathbf{X})\cdot(\mathcal{O}_1\mathbf{X}')]\} = \begin{pmatrix} 4 & 0 & -4 \\ 0 & 0 & 0 \\ -4 & 0 & 4 \end{pmatrix} = 4\begin{pmatrix} 1 & 0 & -1 \\ 0 & 0 & 0 \\ -1 & 0 & 1 \end{pmatrix}. \tag{6}$$

Factors 2 and 4 in equations (5) and (6) indicate the existence of two and four equivalent states $W$ and $K$, respectively. These degenerate states are established by different combinations in the ring connection, as shown in Figure 1(f).

The processes described by equations (5) and (6) are time ordered, and therefore do not commute. It is easy to show that states $W$ and $K$ can only be generated by the order of the operations given in equations (5) and (6), respectively. Namely, the change of the order, i.e.,

$$\mathbf{W} = \mathcal{O}_1[\mathcal{O}_2(\mathbf{X}\cdot\mathbf{X}')] = \mathcal{O}_1\mathbf{Z} \tag{7}$$

is excluded, since $\mathcal{O}_1\mathbf{Z} = 0$, which is an argument in favour to the conclusion about time-ordered processes based on topological arguments.

The matrices of the basic states $X$, $X'$ are regular matrices (Kurepa 1967), i.e

$$\text{Det } \mathbf{X} \neq 0; \quad \text{Det } \mathbf{X}' \neq 0. \tag{8}$$

On the other hand, determinants of derived states $Y$, $Z$, $W$ and $K$, vanish:

$$\text{Det } \mathbf{Y} = 0\text{' Det } \mathbf{Z} = 0; \quad \text{Det } \mathbf{W}' = 0; \text{ Det } \mathbf{K} = 0, \tag{9}$$

indicating that these matrices are singular. Consequently, the columns (rows) of their derived states are linearly dependent (Kurepa 1967).

### 3.2. Case of $P_s \cong P_c$

Consider the case when the momentum transferred from the shock wave to the vortex ring is comparable to the momentum of the circulating fluid. The momentum of the fluid circulation preserves the ring's topology and stability. The transfer of the momentum of the shock wave to the ring causes the additional dissipative process like the ring deformation.

#### 3.2.1. *Deformation before cross-linking*

Low-intensity shock waves may cause deformation of one or both rings by circumferential core deformation, which according to Widnall & Sullivan (1973) appears as a 3-D sinusoidal oscillation [Figure 2(a)]. A more complex case appears when one or both rings are elliptically deformed and, in addition, strongly twisted [Figure 2(b,c)]. Whenever torsional deformation of closely spaced rings was observed, the cross-linking did not take place. In principle, deformation of two vortex rings is a symmetry breaking process which generates a structure of a lower symmetry. In addition, it may even increase their order of topological complexity, thus changing the cross-linking process from the fast into the slow

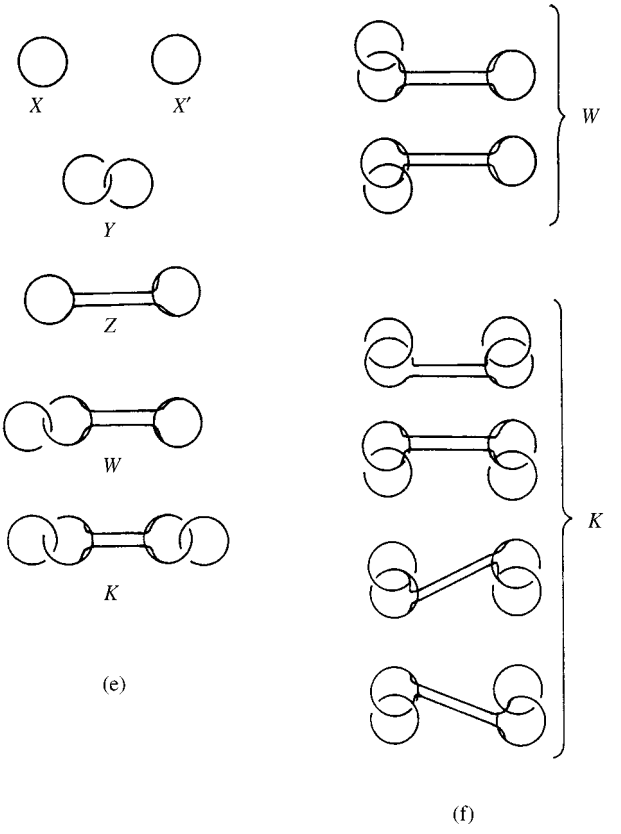


Figure 1 (continued). (e) Schematic representation of the states $X$, $Y$, $Z$, $W$ and $K$. (f) Twofold and fourfold degenerate states $w$ and $K$ defined by the number of possible cross-linkings.

one. If this process takes a longer time than the pulse duration, the cross-linking does not happen. Thus, at a given time scale, deformation of the rings suppresses their cross-linking.

3.2.2. *Deformation during cross-linking*

An interesting type of structure (not reported previously) is shown in Figure 2(d). This structure may be attributed to deformation that coincides with cross-linking in the presence of a turbulent field. Two rings are cross-linked without stretching, which seems to be characteristic of very fast reconnection at low Reynolds numbers. According to Asthurst & Meiron (1987) and as discussed by Pumir & Kerr (1987), every fast reconnection for Reynolds numbers (defined by the ratio $\Gamma/\nu$, of the circulation divided by viscosity) between 100 and 1000 occurs without stretching. A very specific characteristic of the object in Figure 2(d) is the cross-linking which consists of a single tube lying out of the cross-linking plane, actually in the plane perpendicular to it. However, a detailed look on the enlarged and numerically filtered micrograph indicates that the cross-linking tube is not a single one, but two tubes spirally wrapped, with one or perhaps two spiral turns. This cannot be compared with any experimental or numerically generated pattern of reconnection reported in literature. One possible comparison is possibly with the suggestion of Asthurst & Meiron's (1987) that reconnection may occur in a turbulent flow field. In our case the turbulent field

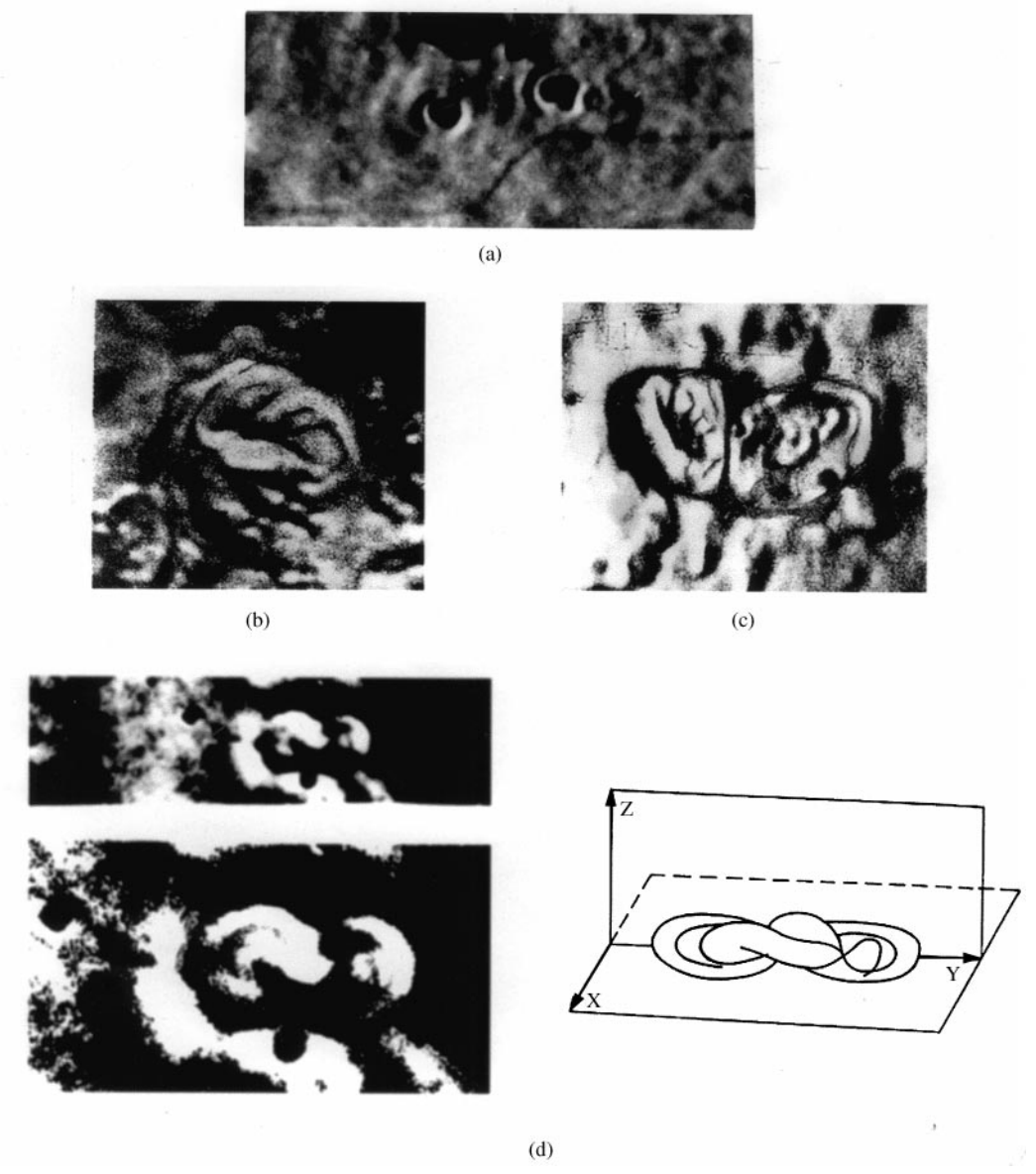


Figure 2. Deformed vortex rings by the shock waves prior to reconnection. (a) Two vortex rings (one deformed by 3-D circumferential oscillation) approach each other. Magnification, $M \sim 1100\times$. (b) One twisted and elliptically deformed vortex ring; $M \sim 1800\times$. (c) Two twisted and elliptically deformed rings at distance $d < \sigma$ (smaller than the core size), which do not undergo cross-linking. Tiny sharp line separating the two rings is clearly seen; $M \sim 1800\times$. (d) The cross-linked rings with the short leg-tubes. Magnification and numerical filtering reveal that the leg-tubes are spirally wrapped as shown on schematic illustration.

(local) is caused by weak shock waves. According to this speculation and calculations done for the circulation ratio of 2:1, the two tubes are spirally wrapped. This occurs in the presence of axial flow associated with tube stretching. However, the tube stretching does not occur in our case, and a doubt remains whether if the interpretation of Asthurst & Meiron (1987) is (completely) applicable to the case observed.

3.2.3. *Deformation after cross-linking*

Deformation of the vortex structures may occur if the shock wave strikes the rings after cross-linking, through deformation of the cross-linking tubes ("legs"), which can be seen in Figure 3(a). Magnification and numerical filtering reveal that the legs connecting rings are deformed by buckling caused by axial compression.

The shock waves may even cause a core collapse by a large spreading of the cross-linking tubes ("legs"), as shown in Figure 3(b). The core spreading of about three times of the initial core size takes place tangentially to the line of discontinuity, which may be assumed to be a shock front, and which is almost normal to the tube "legs". According to Erlbacher *et al.* (1991) when the shock is normal to the vortex axis, a deceleration of the vortex which may lead to its breakdown takes place. A large core spreading indicates a very fast (abrupt) deceleration of fluid (in comparison with a slow core spreading caused by the viscous

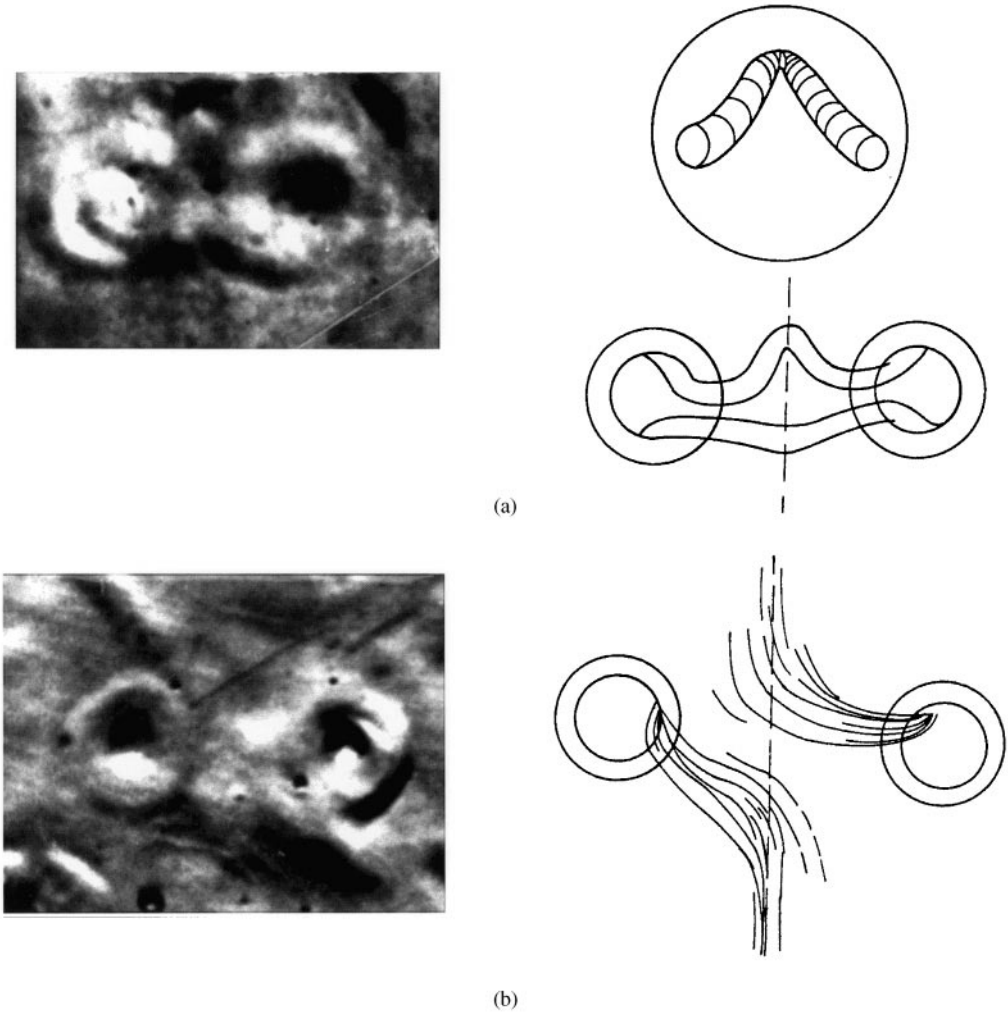


Figure 3. Deformation of the cross-linked structures. (a) Bedding of the tubular legs. Magnification, $M \sim 2300\times$. View of the tube at the buckling point, and schematic diagram. (b) Deformation (and collapse of the tubular legs between cross-linked rings, with diffusive spreading. Magnification ($M \sim 2300\times$)) and schematic reconstruction of the process.

effects). The process which leads to spreading of the core vorticity turns every vortex tube in the opposite direction because of their antiparallel vorticity. However, notice that the bridges [see description of Kida *et al.* (1989)] stay unaffected.

### Case of $P_S > P_C$

Very strong shock waves may cause either violent motion of one ring toward another one at rest as shown in Figure 4(a), or the acceleration of two rings and their collision (by he shocks from opposite sides) as shown in Figure 4(b). These rings approach each other under an angle of $\sim 23^\circ$ what according to Fohl & Turner (1988) this leads to a "double ring formation" i.e., to reconnection. Since the rings collide with great velocity this process is accompanied by a series of successive phenomena, summarized in (i)–(v) in the following.

(i) Interaction of the rings with shock waves opens the possibility for momentum transfer, and consequently for a change of the circulation, $\Gamma$, of the vorticity $\omega$, etc. This manifests itself as core thickening, which occurs on the *same* (right) side of the cross-linked rings [Figure 4]. Similarly, the core thinning occurs on the left side of both rings [Figure 4]. Thus, the core thickening and thinning seem to occur simultaneously on opposite sides of the rings. Magnification and numerical filtering reveal more details of this structure, [Figure 4(c)].

(ii) Shortening of the cross-linking legs as a consequence of the axial compression of the shocks can be seen in Figure 4(b). These legs are much shorter than the legs of the cross-linked rings in the absence of the shock waves.

(iii) Backward reflection of the shock waves from both sides of the cross-linked rings causes a ripple pattern with a characteristic phase shift [Figure 4(b)].

(iv) Generation of singularities in vorticity and of the nodal shape of the core of both rings can be seen in Figure 4(b). Numerical study of the vortex ring reconnection by Asthurst & Meiron (1987) has shown that the nodal shape appears through a singularity in the core vorticity. They have found that distortion of the filament only occurs over an arc which is less than 10% of the initial ring circumference. The small arc segment is frozen in time, i.e., the arc length within this region grows, with a resultant reduction in core size to conserve the vorticity volume. Then self-similar growth pattern appears in the form of modules along the filament generated at points where the axial strain is zero. This type of dynamics leads to singularity in finite time as described by Sigia & Pumir (1985).

Figure 4(c) indicates that singularities in the core vorticity caused by the shock waves take place after ring reconnection. Both rings are shrunk to zero vorticity at singular points, giving rise to a relatively small number of arc segments of vorticity. Distortion of the core is significant and occurs on all segments regardless of their length or curvature. Therefore, thickness of the segment core is not constant but varies along its length what indicates the presence of oscillations in the core. This further indicates that a vortex ring during interaction with the shock wave is not frozen, i.e., its core size, $\sigma$, changes in time very fast and causes the volume vorticity not to be necessary conserved.

(v) In contrast to the case studied by Asthurst & Meiron (1987), Figure 4(c) indicates that a real break occurs in all nodal points of both rings. Broken segments are separated from each other and moved from their position, thus disturbing the circular geometry of the rings. The largest arc segment is strongly bent towards the centre on the same (right) side of both rings. This bending of the arc segment was not observed previously, neither experimentally nor in numerical simulations.

The volume of the broken segments, $V$, (the fragmented vorticity volume), was found by measurement of the length of the arc segments, $s$, and of the core diameter, $\sigma$. Measurements of $\sigma$ have been done at three positions on every segment and the average values were used.

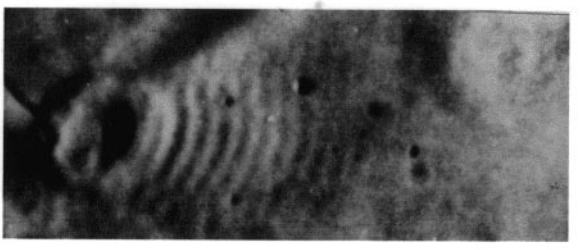

(a)

(b)

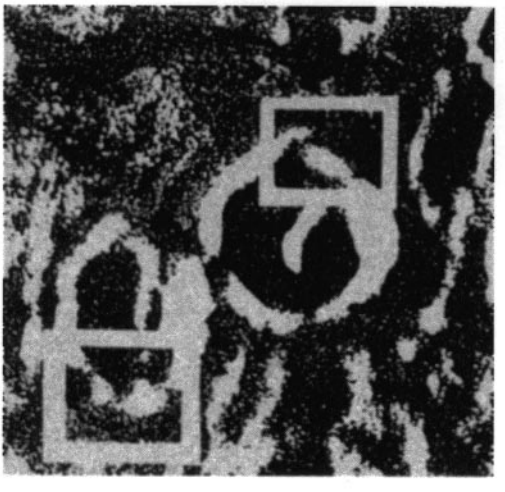

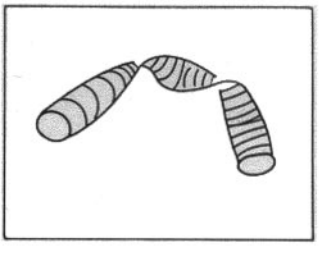

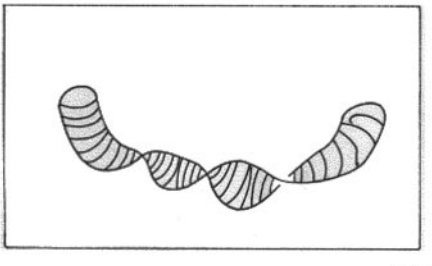

(c)

Figure 4. Collision of two vortex rings by strong shock waves. (a) Acceleration of one ring toward another one at rest; $M \sim 2300\times$. (b) Collision of two accelerated rings at a angle of $\sim 23^{\circ}$; $M \sim 1100\times$. (c) Magnification and numerical filtering reveals a details of the broken rings into arc segments. Schematic illustration represents the arc segments separated by nodal points of singularity.

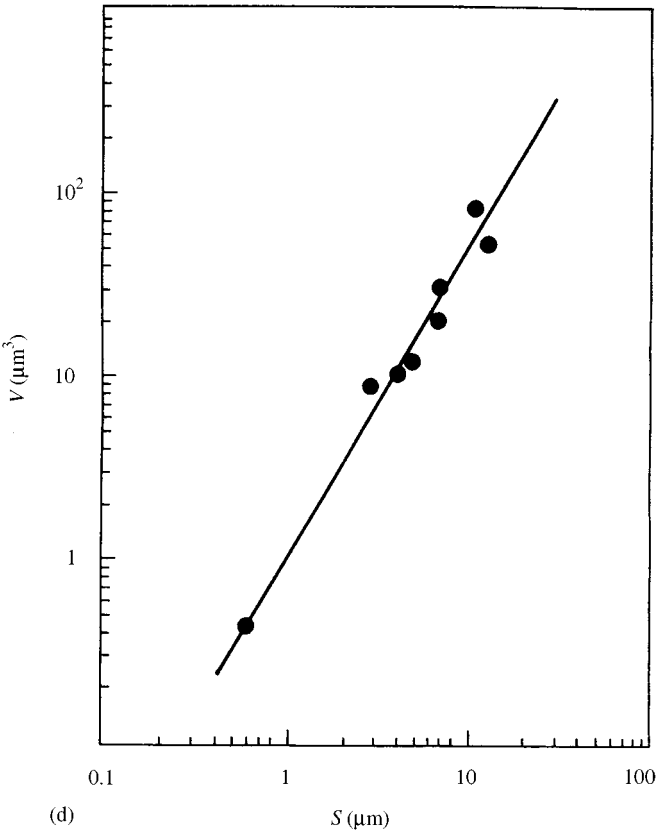


Figure 4 (continued). (d) Log–log plot of the volume vorticity of broken segments of the length $s$.

Figure 4(d) gives the volume, $V$, as a function of the length of the segment $s$, and suggests a dependence of the type

$$V \propto s^D, \tag{10}$$

where $D$ is the slope of the log-log plot: $D \approx 1{\cdot}66 = \frac{5}{3}$. The exponent, $D$, is the fractal dimension of the ring breaking into segments of vorticity, caused by the shock waves.

This seems to be one of the first observations of vortex ring fragmentation under direct impact by a shock wave. It reveals that the vortex ring gets broken into pieces of arc-type filaments which still keep their vorticity. No (significant) diffusion spreading caused either by the shock wave, or by the viscous interaction with the background fluid, is seen. This indicates the existance of "hard core" vorticity, similar to the case of breaking the braided vortex filaments into pieces by the strong shock generated by $Q$-switched ruby laser at $\tau = 24$ ns (Lugomer & Pedarnig 1997).

Increasing the time scale of the interaction (longer pulse duration) to above 30 ns seems to result in structures that cannot be identified (reorganized) because of core spreading via viscous interaction with the background fluid.

The time scale of 10 ns at which the vortex ring interactions were studied, is $\sim 10^5$ times shorter than the scale of Oshima & Izutsu (1988) — to our knowledge the shortest time scale reported up to now. These experiments have demonstrated that a complete vortex ring reconnection process may occur even on an extremely short time-scale, thus positively

answering the question that arose in the literature in this connection. These experiments have also demonstrated the existence of a reach spectrum of dynamical phenomena (associated with the ring reconnection), of a higher topological complexity than in the absence of shock waves.

## 4. CONCLUSION

Vortex rings generated by the bubble explosion in LMI at a short time-scale are put in motion by the surface shock waves. Transfer of momentum from the shock waves to the rings causes their collision and reconnection. All cases observed on $10^{-8}$ s scale are classified into three dynamical regimes on the basis of the relative relation of the $P_S$ with respect to the $P_C$. Summarizing the characteristics of these regimes it can be said that an increase in $P_S$ (momentum transferred to the rings) causes additional dissipative processes on the ring, such as bifurcation, torsion, etc., which in general, hinders the reconnection process. In cases when the hindering becomes large (in comparison with pulse duration), the reconnection may be completely suppressed.

It was shown that the effects of the shock waves on the reconnection process depend not only on the momentum transferred to the rings, but also on the time correlation between the moment of the shock arrival and the time (stage) of the reconnection process (before beginning of reconnection, during reconnection, or after reconnection). It was also shown that very large shock intensity (large $P$ momentum transfer) causes ring instability (the first condition of Tamura is not fulfilled), and its fragmentation into pieces, which has a fractal nature.

For description of the reconnection process of the vortex rings, the matrix formalism is introduced. Assuming the unknotted knots (vortex rings), the knotted knots (Hopf link) the reconnected rings and their combinations to be the states, all the processes that give rise to these structures are assumed to be transformations from one state to another. The matrix formalism enables the transition from one state to another to be described by the action of the particular operator on the matrix of the particular state. This description automatically gives the time ordering of the processes.

## ACKNOWLEDGEMENTS

The author is grateful to Prof. T. Živković, Ruđer Bošković Institute, for stimulating discussions relating to the matrix formalism and to Dr K. Furić for the numerical filtration of the micrographs.

## References

Asthurst, W. T. & Meiron, D. I. 1987 Numerical study of vortex reconnection. *Physical Review Letters* **58,** 1632–1635.

Erlebacher, G., Hussaini, M. Y. & Shu, C. W. 1991 Interaction of a shock wave with longitudinal vortex. Report NASA Langley Research Center, Hampton, VA 23681-0001 (preprint).

Fohl, T. & Turner, J. S. 1975 Colliding vortex rings. *Physics of Fluids* **18,** 433–436.

Glezer, A. 1988 The formation of vortex rings. *Physics Fluids* **31,** 3532–3542.

Jones, V. F. R. 1990 Knot theory and statistical mechanics. *Scientific American* **263,** 52–57.

Kida, S., Takaoka, M. & Hussain, F. 1989 Reconnection of two vortex rings. *Physics Fluids* **A1,** 630–632.

Kurepa, S. 1967 *Finite Dimensional vector spaces and their applications.* Zagreb: Tehnička knjiga (in Croatian).

Lugomer, S. 1996 Observation of laser-induced microscale knotted and unknotted vortex filaments on vapourizing tantalum surface. *Physical Review* **B 54,** 4488–4491.

Lugomer, S. & Maksimović, A. 1997 Solitons on vortex filaments generated by ns laser pulse on metal surface. *Journal of Applied Physics* **82,** 1374–1383.

Lugomer, S. 1998a Observation of solitons on vortex filament bush. *Physics Letters* A **242,** 319–325.

Lugomer, S. 1998b Observation of laser-induced cellular organization of vortex filaments, spatial period doubling and transition to chaos. *Journal of Applied Physics* **83,** 510–517.

Lugomer, S. & Pedarnig, J. D. 1997 Self-organization of vortex filament structures generated in pulsed-laser melting of rough metal surfaces. *Philosophical Magazine* B**75,** 701–732.

O'Keefe, J. D., Skeen, C. H. and York, C. M. 1973 Laser-induced deformation modes in thin metal targets. *Journal of Applied Physics* **44,** 4622–4626.

Oshima, Y. & Izutsu, N. 1988 Cross-linking of two vortex rings. *Physics of Fluids* **31,** 2401–2403.

Pumir, A. & Kerr, R. M. 1987 Numerical simulation of interacting vortex tubes. *Physical Review Letters* **58,** 1636–1639.

Reed, H. L. 1988 Gallery of fluid motion. *Physics of Fluids* **31,** 2383–2394.

Ricca, R. L. & Berger, M. A. 1996 Topological Ideas and fluid mechanics. *Physics Today*, PP. 28–34.

Samokhin, A. A. 1988 First order phase transitions under absorption of laser radiation in condensed matter. In *Absorption of Laser Radiation in Condensed Matter*. Trudi IOFAN, Academy of Sciences USSR (ed. V. B. Fedorov,), pp. 3-98. Moscow: Nauka (in Russian).

Samokhin, A. A. & Uspensky, A. B. 1977 Influence of spinodal characteristics on the evaporation of superheated fluid. *Zhurnal Eksperimentalnoj i Teoretičeskoj Fiziki* **73,** 1025–1031 (in Russian).

Sigia, E. D. & Pumir, A. 1985 Incipient singularities in the Navier–Stokes equations. *Physical Review Letters* **55,** 1749–1752.

Tamura, I. 1976 *Topology of Foliation*. Moscow: MIR Publishers (in Russian: translated from Japanese).

Widnall, S. E. & Sullivan, J. P. 1973 On the stability of vortex rings. *Proceedings of the Royal Society* (London), A **332,** 335–353.

Wu, F. W. 1992 Knott theory and statistical mechanics. *Reviews of Modern Physics* **64,** 1099–1131.